CONSTRAINTS ON THE HIGGS-BOSON TOTAL WIDTH USING $H^*(126) \to ZZ$ EVENTS

R. COVARELLI, for the CMS collaboration
Department of Physics and Astronomy, University of Rochester, 14627, Rochester, NY, United States

Constraints are set on the Higgs boson decay width, Γ_H, using off-shell production and decay to ZZ in the four-lepton (4ℓ), or two-lepton-two-neutrino ($2\ell 2\nu$) final states. The analysis is based on the data collected in 2012 by the CMS experiment at the LHC, corresponding to an integrated luminosity $\mathcal{L} = 19.7\,\text{fb}^{-1}$ at $\sqrt{s} = 8\,\text{TeV}$. A maximum-likelihood fit of invariant mass and kinematic discriminant distributions in the 4ℓ case and of transverse mass or missing energy distributions in the $2\ell 2\nu$ case is performed. The result of it, combined with the 4ℓ measurement near the resonance peak, leads to an upper limit on the Higgs boson width of $\Gamma_H < 4.2 \times \Gamma_H^{SM}$ at the 95% confidence level, assuming $\Gamma_H^{SM} = 4.15\,\text{MeV}$.

1 Introduction

After the discovery of a particle consistent with the standard model (SM) Higgs boson, direct constraints on the new boson width (Γ_H) of 3.4 GeV at the 95% confidence level (CL) have been reported by the CMS experiment in the 4ℓ decay channel [1]. With the current data, the sensitivity for a direct width measurement at the resonance peak is therefore far from the SM Higgs boson expected width of around 4 MeV.

It has been proposed [2] to constrain the Higgs boson width using the off-shell production and decay in ZZ, since, in the gluon-gluon fusion production mode, the off-shell production cross section has been shown to be sizable at high ZZ invariant mass (m_{ZZ}) [3,4].

The production cross section as a function of m_{ZZ} can be written as:

$$\frac{d\sigma_{gg\to H\to ZZ}}{dm_{ZZ}^2} \propto g_{ggH}^2 g_{HZZ}^2 \frac{F(m_{ZZ})}{(m_{ZZ}^2 - m_H^2)^2 + m_H^2\Gamma_H^2}\,, \tag{1}$$

where g_{HZZ} (g_{ggH}) represent the (effective) couplings of the Higgs boson to Z bosons (gluons), m_H is the measured Higgs pole mass, and $F(m_{ZZ})$ is a function which depends on the Higgs boson production and decay amplitudes. In the on-shell (off-shell) regions, the integrated (differential) cross sections are respectively:

$$\sigma_{gg\to H\to ZZ}^{on-shell} = \frac{\kappa_g^2\kappa_Z^2}{r}(\sigma\cdot\mathcal{B})_{SM} \equiv \mu(\sigma\cdot\mathcal{B})_{SM}, \tag{2}$$

and:

$$\frac{d\sigma_{gg\to H\to ZZ}^{off-shell}}{dm_{ZZ}} = \kappa_g^2\kappa_Z^2 \cdot \frac{d\sigma_{gg\to H\to ZZ}^{off-shell,SM}}{dm_{ZZ}} = \mu r \frac{d\sigma_{gg\to H\to ZZ}^{off-shell,SM}}{dm_{ZZ}}, \tag{3}$$

where $(\sigma\cdot\mathcal{B})$ is the cross section times branching fraction to ZZ, all quantities are expressed as adimensonal ratios to their SM values ($\kappa_g = g_{ggH}/g_{ggH}^{SM}$, $\kappa_Z = g_{HZZ}/g_{HZZ}^{SM}$, $r = \Gamma_H/\Gamma_H^{SM}$), and the quantity μ defined by this relationship is referred to as the "signal strength". From Eqs. (2,

3) it is clear that the ratio of off-shell and on-shell production and decay rates in the $H \to ZZ$ channel leads to a direct measurement of Γ_H as long as the ratio of coupling constants remains invariant at the low and high m_{ZZ} values. A similar formalism can be used for the vector boson fusion (VBF) production.

We obtain an upper bound on Γ_H from the comparison of off-shell production and decay distribution in the $H \to ZZ \to 4\ell$ and $H \to ZZ \to 2\ell 2\nu$ channels, and the 4ℓ on-shell rate, where $\ell = e, \mu$. The analysis is based on the dataset collected by the CMS experiment during the 2012 LHC running period, which corresponds to an integrated luminosity of 19.7 fb^{-1} of pp collisions at a center-of-mass energy of $\sqrt{s} = 8$ TeV. Details of this analysis can be found in [5,6]. A detailed description of the CMS detector can be found in Ref. [7]. Concerning lepton and missing transverse energy reconstruction and event selection, this analysis uses the same algorithms as in Refs. [1,8].

2 Analysis strategy

As shown above, once a value of μ is constrained from an independent measurement or calculation, the off-shell cross section as a function of m_{ZZ} is proportional to Γ_H. We use two different assumptions for μ, i.e. the measured value from the the 4ℓ on-shell analysis [1], or $\mu = 1$ assuming the SM expectations in the peak, with the expected uncertainties from the same analysis.

The VBF mechanism also leads to significant off-shell Higgs production. The signal strengths can be considered separately for the gluon-gluon fusion (μ_F) and VBF (μ_V) production mechanisms. However, because of the limited precision obtained on these quantities from the current data, we assume in this analysis that $\mu_V = \mu_F = \mu$.

At large m_{ZZ}, interference between signal and background for the processes with the same initial and final states is not negligible and must be taken into account. Therefore the event likelihood can be written as:

$$\begin{aligned}\mathcal{P}^{\text{off-shell}}_{\text{tot}}(\vec{x}) = &\left[\mu r \times \mathcal{P}^{gg}_{\text{sig}}(\vec{x}) + \sqrt{\mu r} \times \mathcal{P}^{gg}_{\text{int}}(\vec{x}) + \mathcal{P}^{gg}_{\text{bkg}}(\vec{x})\right] + \\ &+ \left[\mu r \times \mathcal{P}^{\text{VBF}}_{\text{sig}}(\vec{x}) + \sqrt{\mu r} \times \mathcal{P}^{\text{VBF}}_{\text{int}}(\vec{x}) + \mathcal{P}^{\text{VBF}}_{\text{bkg}}(\vec{x})\right] + \mathcal{P}^{q\bar{q}}_{\text{bkg}}(\vec{x}) + (\text{other backgrounds}) \quad (4)\end{aligned}$$

where $\mathcal{P}_{\text{sig}}$, $\mathcal{P}_{\text{int}}$ and $\mathcal{P}_{\text{bkg}}$ are signal, interference, and background probability functions, respectively, for gluon-gluon fusion and VBF production, and defined as functions of the variables used in each analysis.

3 Monte Carlo simulation

The Monte Carlo (MC) samples used in this analysis are the same as those described in Refs. [1] and [8].

Additionally, $gg \to 4\ell$ ($2\ell 2\nu$) events, as well as $qq' \to ZZqq' \to 4\ell qq'$ ($2\ell 2\nu qq'$) VBF events, have been generated at the leading order (LO) including the Higgs signal as well as the background and interference using different MC generators: GG2VV 3.1.5 [4,9], MCFM 6.7 [10,11], and PHANTOM [12]. Samples have been generated with MSTW2008 LO parton density functions (PDFs) and the renormalization and factorization scales are proportional to m_{ZZ} ("running" scales).

We apply to next-to-next-to-leading order (NNLO) corrections ("K-factors") as a function of m_{ZZ} [13] to the gluon-fusion signal process and, even if exact calculations of the background process are limited to LO, we assign the same K-factor to it, relying on soft-collinear approximation [14]. For VBF production, the event yield is normalized to the cross section at NNLO [15], with a normalization factor independent of $m_{4\ell}$.

4 $H \to ZZ \to 4\ell$ analysis

In addition to the reconstruction, selection, and analysis methods developed in [1], the 4ℓ off-shell analysis uses a dedicated kinematic discriminant $\mathcal{D}_{gg}$ which describes the production and decay dynamics in the ZZ center-of-mass frame using as observables the two dilepton masses as well as five independent angles [16]. The discriminant is defined as $\mathcal{D}_{gg,a} \equiv \mathcal{P}_{gg,a}/(\mathcal{P}_{gg,a} + \mathcal{P}_{q\bar{q}})$, where $\mathcal{P}_i$ is the probability for a 4ℓ event to come either from $gg \to ZZ$ or $q\bar{q} \to ZZ$ processes. The discriminant is defined for a signal-weight parameter a, where $a = 1$ corresponds to the SM. We set $a = 10$ in constructing the discriminant, since an exclusion of the order of $r = 10$ is expected to be achieved. Figure 1 shows the distribution of the the 4ℓ invariant mass (left) and the $\mathcal{D}_{gg}$ variable (center) for all expected contributions, as well as for the data.

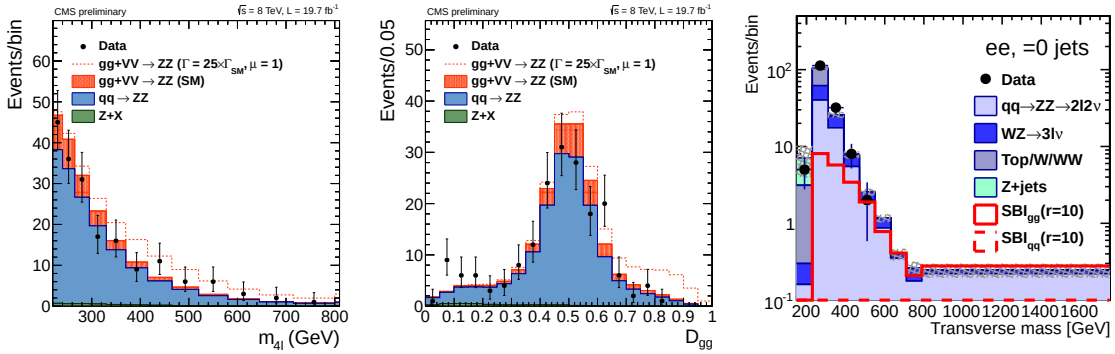

Figure 1 – Distributions of the discriminating variables used in the 4ℓ analysis: $m_{4\ell}$ (left) and $\mathcal{D}_{gg}$ (center) for the data and all the expected contributions. The latter are shown for the SM expectation, as well as for an hypothesis corresponding to $r = 25$, and include both the gg and the VBF processes. Distribution of the m_T variable (right) in the in the $2e2\nu$ 0-jet category, for the data and the expected contributions. The shapes of gg and VBF inclusive processeses (SBI = signal, background and interference) for a $r = 10$ scenario are superimposed.

5 $H \to ZZ \to 2\ell 2\nu$ analysis

Following the same event reconstruction and selection used in previous searches for high-mass Higgs bosons [8], the selected events are split according to lepton flavors (e and μ) and jet categorization (0 jets, $\geq$1 jet, and "VBF-like", i.e. two jets satisfying $m_{jj} > 400$ GeV and $\Delta\eta_{jj} > 4$). The transverse mass (m_T) distributions for the 0 and $\geq$1 jets categories and the missing transverse energy (E_T^{miss}) distribution for the VBF-like category are used as final discriminant variables. The m_T variable is defined as follows:

$$m_T^2 = \left[\sqrt{p_{T,\ell\ell}{}^2 + m_{\ell\ell}{}^2} + \sqrt{E_T^{miss\,2} + m_{\ell\ell}{}^2}\right]^2 - \left[\vec{p}_{T,\ell\ell} + \vec{E}_T^{miss}\right]^2 \quad (5)$$

where $\vec{p}_{T,\ell\ell}$ and $m_{\ell\ell}$ are the measured transverse momentum and invariant mass of the dilepton system, respectively. One of the m_T distributions is shown in Fig. 1 (right).

6 Systematic uncertainties

The main systematic uncertainty in this analysis comes from the measured value of μ: in the approach using its expected (observed) value, it is taken from Ref. [1] to be $1.00^{+0.27}_{-0.24}$ ($0.93^{+0.26}_{-0.24}$). In the approach used in this analysis, all signal systematics for the 4ℓ final state depending only on normalization cancel when using the measured on-shell signal strength as a reference. Other experimental systematic uncertainties are considered on the amount of reducible background in the 4ℓ analysis and in the evaluation of $E_T^{miss}$and the b-jet veto efficiency in the $2\ell 2\nu$ analysis.

Theoretical uncertainties are important in this analysis for the signal and interference contributions and for the $q\bar{q} \to ZZ$ background. QCD renormalization and factorization scales are varied by a factor two both up and down, and uncertainties from PDF variations are extracted by changing PDF sets. These uncertainties are computed on LO MC and K-factors and applied consistently. To account for the limited knowledge on the gg $\to$ ZZ continuum background cross section at NNLO (and therefore on the interference), we assign an additional systematic uncertainty of 10%.

7 Results

Using the normalization and shape of the signal and background distributions, which are derived either from MC or control samples, an unbinned maximum-likelihood fit of the data is performed, where systematic uncertainties are included as nuisance parameters. In the 4ℓ analysis the kinematic discriminant is combined with $m_{4\ell}$ in a two-dimensional fit, while m_{T} or $E_{\mathrm{T}}^{\mathrm{miss}}$ distributions are used for the $2l2\nu$ channel. Fit results are shown in Fig. 2, in the form of negative log-likelihood scans as a function of r. The red dashed lines correspond to 68% and 95% CL exclusion values. Table 1 shows the results obtained using the observed value of μ. Combination of the two channels results in an observed (expected) exclusion of $\Gamma_{\mathrm{H}} \leq 4.2\ (8.5) \times \Gamma_{\mathrm{H}}^{\mathrm{SM}}$ at the 95% CL, or $\Gamma_{\mathrm{H}} \leq 17.4\ (35.3)$ MeV.

	4ℓ	$2\ell2\nu$	Combined
Expected 95% CL limit, r	11.5	10.7	8.5
Observed 95% CL limit, r	6.6	6.4	4.2
Observed 95% CL limit, Γ_{H} (MeV)	27.4	26.6	17.4
Observed best fit, r	$0.5\ ^{+2.3}_{-0.5}$	$0.2\ ^{+2.2}_{-0.2}$	$0.3\ ^{+1.5}_{-0.3}$
Observed best fit, Γ_{H} (MeV)	$2.0\ ^{+9.6}_{-2.0}$	$0.8\ ^{+9.1}_{-0.8}$	$1.4\ ^{+6.1}_{-1.4}$

Table 1: Expected and observed 95% CL limits and fitted values of r or Γ_{H} for the 4ℓ analysis, the $2\ell2\nu$ analysis and for the combination, using the observed value of μ.

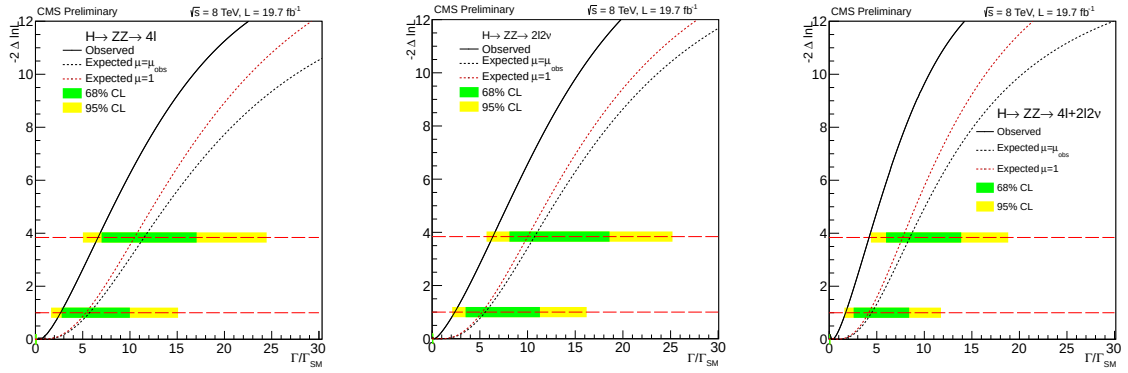

Figure 2 – Negative log-likelihood scans as a function of $r = \Gamma_{\mathrm{H}}/\Gamma_{\mathrm{H}}^{\mathrm{SM}}$ for the 4ℓ (left) and $2\ell2\nu$ (center) analyses separately and for the combined result (right). Green and yellow bands correspond respectively to 68% and 95% quantiles of the distribution of the negative log-likelihood at the corresponding value on the red line, using MC pseudo-experiments.

References

1. S. Chatrchyan *et al* (CMS collaboration), *Phys. Rev.* D **89**, 092007 (2014).
2. F. Caola and K. Melnikov, *Phys. Rev.* D **88**, 054024 (2013).
3. G. Passarino, *JHEP* **08**, 146 (2012).
4. N. Kauer and G. Passarino, *JHEP* **08**, 116 (2012).

5. S. Chatrchyan *et al* (CMS collaboration), CMS-PAS-HIG-14-002 (2014), http://cds.cern.ch/record/1670066.
6. https://twiki.cern.ch/twiki/bin/view/CMSPublic/Hig14002TWiki.
7. S. Chatrchyan *et al* (CMS collaboration), *JINST* **3**, S08004 (2008).
8. S. Chatrchyan *et al* (CMS collaboration), CMS-PAS-HIG-13-014 (2013), http://cds.cern.ch/record/1546776.
9. N. Kauer, proceedings to 10th Int. Sym. on Radiative Corrections (RADCOR2011), PoS RADCOR2011, 027 (2011).
10. J.M. Campbell *et al*, arXiv:1311.3589.
11. J.M. Campbell and R.K. Ellis, *Nucl. Phys. Proc. Suppl.* **205**, 10 (2010).
12. A. Ballestrero *et al*, *Comput. Phys. Commun.* **180**, 401 (2009).
13. G. Passarino, *Eur. Phys. J.* C **74**, 2866 (2014).
14. M. Bonvini *et al*, *Phys. Rev.* D **88**, 034032 (2013).
15. LHC Higgs Cross Section Working Group, CERN-2011-002 report, arXiv:1101.0593.
16. Y. Gao *et al*, *Phys. Rev.* D **81**, 075022 (2010).